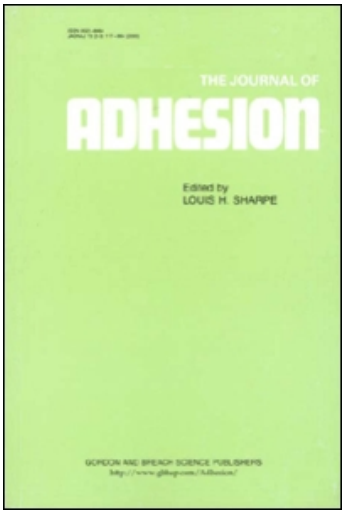

The Journal of Adhesion
Publication details, including instructions for authors and subscription information:
http://www.informaworld.com/smpp/title~content=t713453635

Particle removal mechanisms in cryogenic surface cleaning

Christopher Toscano[a]; Goodarz Ahmadi[a]
[a] Department of Mechanical and Aeronautical Engineering, Clarkson University, Potsdam, New York, USA

Online publication date: 08 September 2010

To cite this Article Toscano, Christopher and Ahmadi, Goodarz(2003) 'Particle removal mechanisms in cryogenic surface cleaning', The Journal of Adhesion, 79: 2, 175 — 201
To link to this Article: DOI: 10.1080/00218460309570
URL: http://dx.doi.org/10.1080/00218460309570

The Journal of Adhesion, 79: 175–201, 2003

0021-8464/03 $12.00 +.00
DOI: 10.1080/00218460390147942

Taylor & Francis
Taylor & Francis Group

PARTICLE REMOVAL MECHANISMS IN CRYOGENIC SURFACE CLEANING

Christopher Toscano
Goodarz Ahmadi
Department of Mechanical and Aeronautical Engineering,
Clarkson University, Potsdam, New York, USA

Particle removal mechanisms in cryogenic surface cleaning are examined. The effect of impacting solid carbon dioxide particles and the hydrodynamic forces and torques are included in the model. Sliding detachment models and rolling detachment models in conjunction with the theory of critical moment are used. The critical conditions for removal of particles of different sizes are evaluated. For various carbon dioxide pellet diameters, incoming flow angles, nozzle, and cleaning surface separation distances, the critical shear velocities for particle detachment are evaluated.

Keywords: Cryogenic cleaning; Particle adhesion; Detachment mechanism; Carbon dioxide snow; Impact detachment

INTRODUCTION

With the numerous problems associated with the wet cleaning process (such as its ineffectiveness for submicron particles, environmental disposal regulation, etc.), there has been increasing interest in the use of cryogenic aerosols for cleaning applications. Cryogenic cleaning is also becoming very important for surface cleaning in the microelectronic and xerographic industries. In this approach, a high-speed jet of

Received 18 January 2002; in final form 30 July 2002.

This work was supported by the New York State Office of Science, Technology and Academic Research (NYSTAR) (through the Center for Advanced Materials Processing, CAMP, of Clarkson University).

Presented in part at the 25th Annual Meeting of The Adhesion Society, Inc., held in Orlando, Florida, USA, 10–14 February 2002.

Address correspondence to Goodarz Ahmadi, Clarkson University, Department of Mechanical and Aeronautical Engineering, P.O. Box 5725, Potsdam, NY 13699-5725. E-mail: ahmadi@clarkson.edu

carbon dioxide or argon is forced through a converging-diverging nozzle. This results in the formation of solid carbon dioxide or argon ice flakes in the diverging part of the nozzle. The presence of solid flakes in the high-speed jet is believed to increase the efficiency of particle removal. Solid flakes have an advantage over more traditional liquid or air cleaning systems. Larger solid particles are able to penetrate directly to the surface, passing through the boundary layer, and remove the contaminant particle by impact detachment or other physical or chemical mechanisms [1, 2].

While the exact mechanisms of cryogenic cleaning are not known, there are several theories presented by Jackson and Carver [3]. One hypothesis is that the carbon dioxide pellets transfer their momentum to the adhered particles by impact and overcome the van der Waals forces [3]. The impulse from the impacting pellets dislodges the adhered particles from the surface. The second hypothesis involves viscous drag separation. The high gas velocity at the surface produces high viscous drag on a surface particle and causes it to be detached. A third hypothesis suggests that the chemical separation and a phase change of minute solid carbon dioxide particles from solid state to liquid state are the underlying mechanisms behind removal. This results in rapid microsolutioning of trace surface residues in liquid carbon dioxide [3]. A fourth hypothesis is that the carbon dioxide pellets evaporate rapidly at the surface. The explosive evaporation blasts the adhered particles away from the surface.

Extensive reviews of particle adhesion mechanisms were provided by Corn [4], Krupp [5], Visser [6], Tabor [7], Bowling [8], Ranade [9], and Soltani and Ahmadi [10]. Accordingly, it is understood that the van der Waals force contribution is significant to the particle adhesion force on a surface under dry conditions. The van der Waals force was evaluated through microscopic and macroscopic approaches [11, 12].

Derjaguin [13] was the first to examine contact deformation using the Hertz model. Johnson, Kendall, and Roberts [14] developed a detailed theory of particle adhesion including the combined effects of deformation and surface energy. Their so-called JKR model of particle adhesion predicts that the contact area remains finite at the moment of separation.

Derjaguin, Muller, and Toporov [15] used the Hertzian contact assumption, and contended that the contact area diminishes at the moment of separation. For particle removal this model (referred to as the DMT theory) requires a force four-thirds as large as the JKR model. Debate over the validity of each of these models has been extensive. Muller *et al.* [16, 17] suggest that the JKR model is more applicable to systems with low Young's modulus, high surface

energies, and small particle diameters, while the DMT model is better suited for systems with high Young's modulus, low surface energies, and large particle diameters.

Hoenig [1, 2] was the first to suggest the prospects of utilizing carbon dioxide for surface cleaning. Hoenig felt that the optimum cleaning system would incorporate a flow of soft particulates over a surface to remove adhered particles. The gas utilized would need to be nontoxic, ultraclean, and low in cost. Carbon dioxide was the only gas that Hoenig found to meet all criteria. Carbon dioxide can be expanded slowly to produce a phase change from gas to solid, thereby creating snowflakes. The resulting snow can be blown across a surface to remove particulate contamination. Hoenig [1, 2] mainly studied the effectiveness of carbon dioxide cleaning in integrated circuits applications. Wadlow [18] studied the application of the carbon dioxide cleaning in vacuum system passages. McDermott *et al.* [19, 20] developed a cryogenic surface cleaning process using argon instead of carbon dioxide. Loveridge [21] utilized the carbon dioxide jet spray to clean infrared thin-coated optics. John *et al.* [22] and John and Sethi [23] studied impact induced by resuspension and the breakup of latex doublets. Kohli [24] has compared the advantages and disadvantages of several nonaqueous cleaning processes. Wang *et al.* [25] adapted the cryogenic carbon dioxide process for chip resistor cleaning. Narayanswami [26] conducted a theoretical analysis of wafer cleaning using cryogenic aerosols.

In this work, a model for particle removal in cryogenic surface cleaning is developed. The theory of critical moment in conjunction with rolling detachment along with sliding detachment models for adhered particles are used. The effect of carbon dioxide pellet impact on adhered particles is included in the removal models. For the cases where the particles follow the boundary layer flow or penetrate through the boundary layer and impact directly, the critical value of the shear velocity for adhered particle detachment is evaluated. Effects of particle size, materials (van der Waals force), impact force, lift force, drag force, and angle of incoming flow are examined.

FORMULATION

The moment and rolling detachment mechanisms, which are important for particle removal by cryogenic fluid flows, are briefly outlined. The hydrodynamic lift, drag, and moment, as well as the impact force of carbon dioxide pellets that act on the adhered particle, are described.

Figure 1 shows the geometric features of a particle adhered to a wall at the moment that a CO_2 pellet collides with it during the

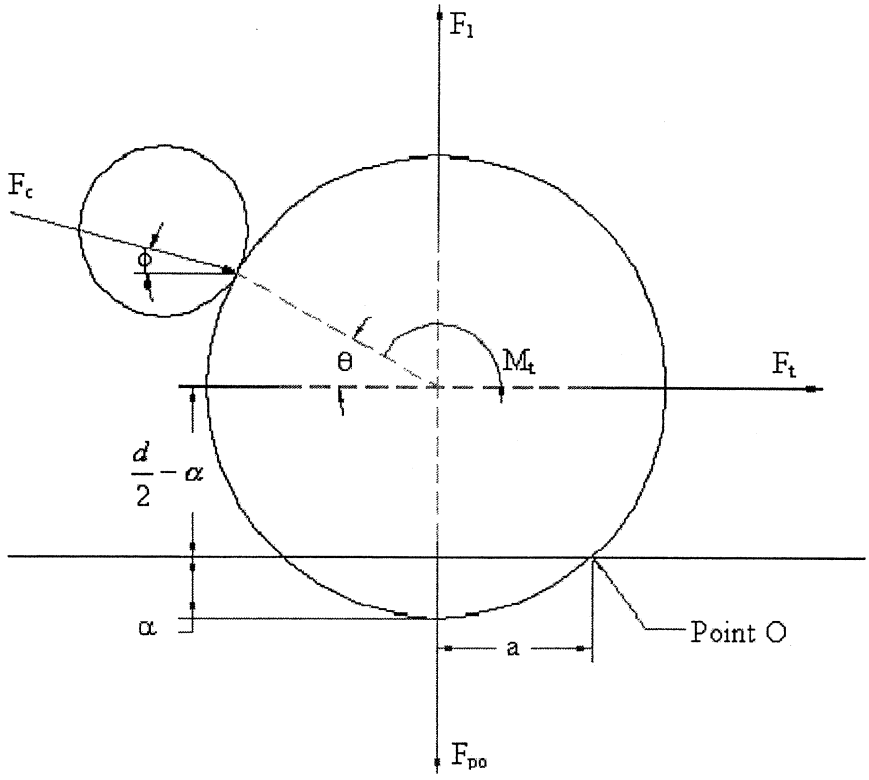

FIGURE 1 Free body diagram of the forces acting on an adhered particle.

cryogenic cleaning process. In this figure, M_t is the hydrodynamic moment acting on the adhered particle, F_t is the drag force, F_l is the lift force, F_c is the impact force due to the collision with the CO_2 pellet, F_{po} is the pull-off force, d_1 is the diameter of the adhered particle, a is the contact radius, α_o is the relative approach between the particle and surface (at equilibrium conditions), θ is the angle of collision relative to the adhered particle, and φ is the angle of approach for the colliding particle. The relative approach is typically very small in comparison with d/2 and neglected in most practical analysis.

Hydrodynamic Torque

The hydrodynamic moment of the viscous stress acting on a particle in contact with a wall is given as

$$M_t = \frac{2\pi\mu b d_1^2 V}{C_c} \tag{1}$$

where V for two-dimensional flows near a wall is given as

$$V = \left(u^2 + w^2\right)^{1/2} \tag{2}$$

Here V is the magnitude of the fluid velocity vector acting at the center of the particle, u and w represent the fluid velocities in the streamwise and spanwise directions, μ is the coefficient of viscosity, and the dimensionless coefficient b ($= 0.944$) is the correction factor for the wall effect as derived by O'Neill [27].

The Cunningham slip correction factor, C_c, is also included in Equation (1) for submicrometer particles. The exact expression for the gas slip effect on hydrodynamic torque for ultra fine particles is not known. The expression given by Equation (1) is used as an approximation. The Cunningham correction factor is given as

$$C_c = 1 + \frac{2\lambda}{d_1}\left[1.257 + .4e^{\frac{-1.1d_1}{2\lambda}}\right] \tag{3}$$

where λ is the mean free path of the fluid.

Drag Force

The Stokes drag force acting on a particle in contact with a surface is given as [27]

$$F_t = \frac{3\pi f \mu d_1 C_d}{C_c} V \tag{4}$$

where f ($= 1.7009$) is the dimensionless coefficient for the wall effect derived by O'Neill. Here the coefficient C_d is added to Equation (4) to account for the nonlinear correction to the Stokes drag at high velocities that is

$$C_d = 1 + 0.15\mathrm{Re}^{0.687} \tag{5}$$

where Re, the Reynolds number, is defined as

$$\mathrm{Re} = \frac{V d_1}{\nu} \tag{6}$$

Here d_1 is the diameter of adhered particle and d_2 is the diameter of impacting particles.

Lift Force

The expression for the Saffman [28] lift force is given as

$$F_l = 1.61 d_1^2 V (\rho\mu)^{1/2} \frac{\frac{dV}{dy}}{\left|\frac{dV}{dy}\right|^{1/2}} \tag{7}$$

The lift force is typically small and may be neglected in the particle detachment, but it was included for this analysis.

Impact Force

The collision force, F_c, results from the impact of the solid carbon dioxide particles within the cryogenic stream with the particles adhered to the surface. The force of collision, F_c, between two particles is given as [29]

$$F_c = \frac{4}{3} E^* \sqrt{r^*} \left(\frac{15 m^* V_{cl}^2}{16 E^* \sqrt{r^*}} \right)^{\frac{3}{5}} \tag{8}$$

Here E^* is the contact modulus, r^* is the effective radius, V_{cl} is the velocity of the incoming carbon dioxide pellets relative to the adhered particle along the line of impact, and m^* is the effective mass.

The contact modulus is the effective Young's modulus for interactions between the adhered and colliding particles. This is given as

$$\frac{1}{E^*} = \frac{1 - {\gamma_1}^2}{E_1} + \frac{1 - {\gamma_2}^2}{E_2} \tag{9}$$

Here E^* is the effective Young's modulus, γ is the Poisson's ratio, and the subscripts 1 and 2 refer to the adhered particle and carbon dioxide pellets, respectively.

The effective radius is defined as the inverse mean of the two radii, *i.e.*,

$$\frac{1}{r^*} = \frac{1}{r_1} + \frac{1}{r_2} \tag{10}$$

Similarly, the effective mass is also the inverse mean of the two particles and is given by

$$\frac{1}{m^*} = \frac{1}{m_1} + \frac{1}{m_2} \tag{11}$$

Adhesion Force

The van der Waals adhesion force results from the interaction of intermolecular forces at the interface. The pull-off force needed to overcome the adhesion force as obtained from the JKR model is given as

$$F_{po}^{JKR} = \frac{3}{4}\pi W_A d_1 \tag{12}$$

Here W_A is the thermodynamic work of adhesion given by

$$W_A = \frac{\mathrm{A}}{12\pi {z_o}^2} \tag{13}$$

where z_o is the minimum separation distance and A is the Hamaker constant. According to the JKR theory, at the moment of separation there is a nonvanishing contact radius, a, which is given as

$$a = \left(\frac{3\pi W_A {d_1}^2}{8K}\right)^{1/3} \tag{14}$$

and the composite Young's modulus, K, is given by

$$K = \frac{4}{3}\left[\frac{\left(1-{\gamma_1}^2\right)}{E_1} + \frac{\left(1-{\gamma_3}^2\right)}{E_3}\right]^{-1} \tag{15}$$

Here E is the Young's Modulus and γ is the Poisson's ratio of the adhered particle and the surface, subscripts 1 and 3, respectively.

Relaxation Time and Impact Velocity

The contaminant particles that are adhered to the surface are not directly exposed to the nozzle velocity. The cryogenic flow will form a boundary layer flow over the substrate with suspended particles in its stream. Figure 2 shows the schematics of the flow pattern. To account for the impact effect of a carbon dioxide pellet on the contaminant particle, the impact velocity of the carbon dioxide particle needs to be estimated. Clearly, the pellet velocity at impact is somewhere between the nozzle velocity and the local gas velocity. The impact velocity is approximately given as

$$\overrightarrow{V}_c = \overrightarrow{V}_o e^{-1/\tau} + V(1-e^{-t/\tau})\overrightarrow{i} \tag{16}$$

where $\overrightarrow{V}_o$ is the nozzle velocity vector, V is the fluid velocity at the level of contaminant particle centroid from the substrate, t is the flight time to impact, and τ is the relaxation time defined as

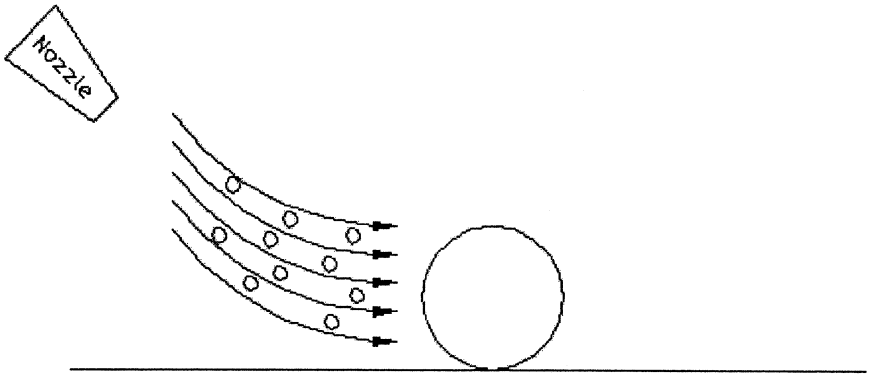

FIGURE 2 Schematics of a flow field near a wall.

$$\tau = \frac{{d_2}^2 \rho^p C_c}{18\mu} \tag{17}$$

Here d_2 and ρ^p are the diameter and density of the solid carbon dioxide particle and μ is the viscosity of the gaseous carbon dioxide. The variation of relaxation time with particle diameters in a carbon dioxide stream at 293 K is shown in Figure 3. Accordingly, the relaxation times for 0.5 μm and 4 μm carbon dioxide particles are 4.5×10^{-6} s and 2.4×10^{-4} s, respectively. Equation (16) shows that the impact velocity becomes comparable with the nozzle velocity for large carbon dioxide particles (with large τ) and short flight times. For small carbon dioxide pellets and large flight times, the particles follow the flow and the impact velocity approaches that of the local gas velocity near the substrate.

Typically the nozzle is at a distance of L = 2 cm from the substrate and the flight time is estimated as $t = L/V_o$. Using Equation (16), the impact velocity of a 0.5 μm particle with $t/\tau \gg 1$ is given by

$$\vec{V}_c = V\vec{i} \tag{18}$$

Similarly, for a 4 μm particle with $t/\tau = 83/V_o$ the impact velocity is given by

$$\vec{V}_c = \vec{V}_o e^{\left(\frac{-83}{V_o}\right)} + V\left[1 - e^{\left(\frac{-83}{V_o}\right)}\right]\vec{i} \tag{19}$$

Equations (18) and (19) imply that a 0.5 μm carbon dioxide pellet will impact the adhered particles at the local fluid velocity, while the 4 μm

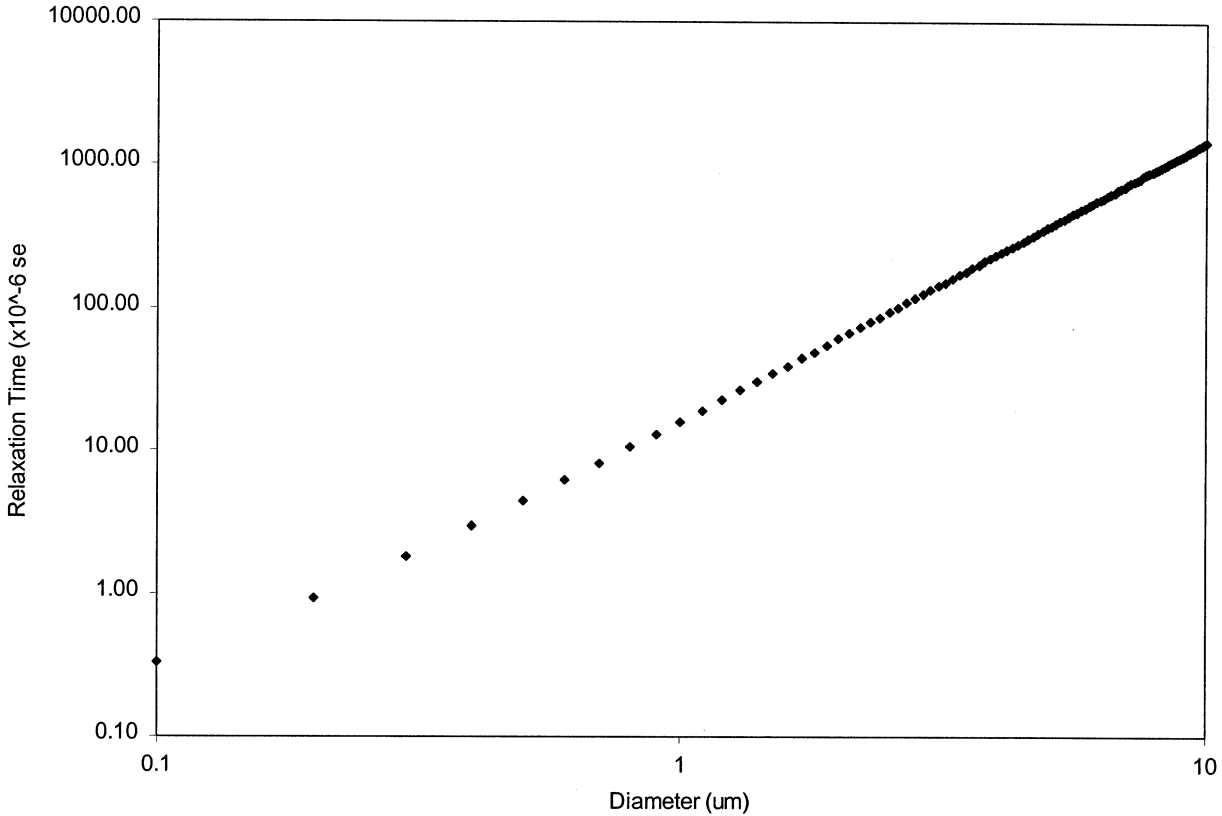

FIGURE 3 Relaxation time for carbon dioxide particles in a carbon dioxide stream at 293 K.

particles will have a substantial fraction of the nozzle velocity. Note that the shear velocity (in turbulent boundary layer) is estimated as

$$u^* \approx \frac{1}{20} \mathrm{V_o} \tag{20}$$

Here it is assumed that the free stream velocity is about the same as the nozzle velocity.

It should be emphasized that Equations (16) and (19) account approximately for the variation of the impact velocity due to the drag retardation of carbon dioxide particles in the turbulent boundary layer near the wall. The effects of shear lift force and details of particle trajectory are, however, neglected in these analyses. Here we also assumed that the CO_2 pellets are spherical in shape. This is consistent with the observation of Kohli [24].

Impact Angle

The velocity components of the carbon dioxide pellets at impact are given as

$$\begin{aligned} V_{cx} &= V_o \cos\phi \; e^{\left(\frac{-t}{\tau}\right)} + V\left[1 - e^{\left(\frac{-t}{\tau}\right)}\right] \\ V_{cy} &= V_o \sin\phi \; e^{\left(\frac{-t}{\tau}\right)} \end{aligned} \tag{21}$$

Here ϕ is the nozzle angle with the horizontal direction. The velocity along the line of impact, V_{cl}, is given by

$$V_{cl} = V_{cx} \cos\theta + V_{cy} \sin\theta \tag{22}$$

where θ, the impact angle of the carbon dioxide pellet with the contaminant, is given as

$$\tan\theta = \frac{V_{cx}}{V_{cy}} \tag{23}$$

For large particles and short travel time (large nozzle velocity), when $t/\tau \ll 1$ the impact angle is approximately equal to the nozzle angle. However, if the carbon dioxide pellets are larger than the contaminant the impact angle given by Equation (23) may not be possible due to the geometric constraint shown in Figure 4. In this case the impact angle is corrected to the minimum impact angle possible. From Figure 4, the minimum angle at which a larger carbon dioxide pellet can impact a smaller contaminant particle is given as

$$\sin\theta = \frac{d_2 - d_1}{d_2 + d_1} \tag{24}$$

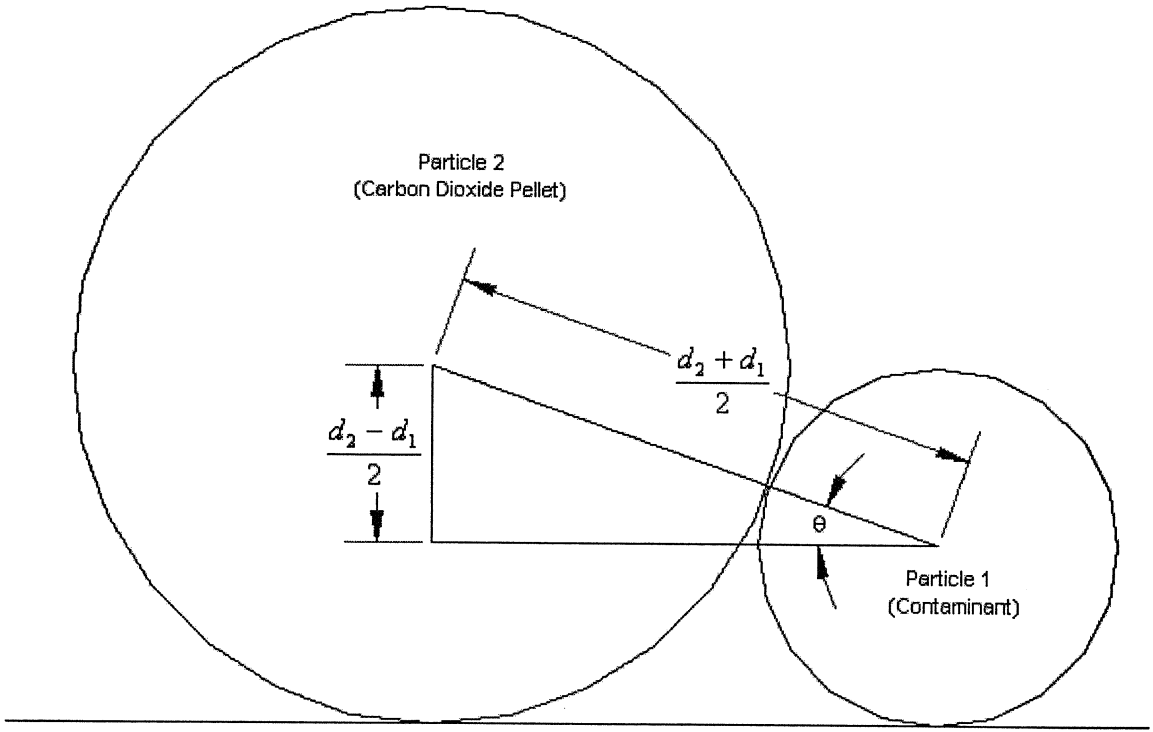

FIGURE 4 Minimum angle of impact for a larger carbon dioxide particle colliding with a smaller contaminant.

Here d_1 and d_2 are, respectively, the diameter of contaminant particle and carbon dioxide pellet.

Rolling Particle Detachment

Tsai *et al.* [30] and Soltani and Ahmadi [10] described the critical moment model criteria for rolling particle detachment. Accordingly, when the external moment becomes greater than or equal to the resisting moment due to the adhesion force, the adhered particle will roll from its equilibrium position and is detached from the surface.

The lift, drag, and impact forces and the hydrodynamic moment acting on the adhered particle and their lines of action are shown in Figure 1. The moments created by the lift, drag, and impact forces, in addition to the hydrodynamic moment, overcome the moment created by the adhesion force leading to particle removal. With respect to point O, the criterion for the detachment of the particle is given as

$$M_t + F_t\left(\frac{d_1}{2}\right) + F_l a + F_c\left[-(\sin\theta)\left(\frac{d_1}{2}\cos\theta + a\right) + (\cos\theta)\left(\frac{d_1}{2}\sin\theta + \frac{d_1}{2}\right)\right] \geq F_{po}a \tag{25}$$

At the moment that the inequality in Equation (25) holds, the contaminant particle will roll from its equilibrium position and is then assumed to be detached.

Sliding Particle Detachment

Wang [31] and Soltani and Ahmadi [10] described the necessary criteria for sliding particle detachment. The particle will be removed by sliding detachment if the frictional force is overcome. That is,

$$F_t + F_c\cos\theta \geq \left(F_{po} - F_l + F_c\sin\theta\right)k \tag{26}$$

Here $F_c\cos\theta$ is the component of the impact force acting parallel to the surface, $F_c\sin\theta$ is the impact force component perpendicular to the surface, and k is the static coefficient of friction. Whenever the criterion in Equation (26) is satisfied, the contaminant particle slides and is assumed to be detached from the substrate.

SUBLAYER FLOW

It is known that the turbulent near wall flows contain coherent axial eddies that are spaced at about 100 wall units. These vortices generate

high and low speed streaks near the surface. Vortical motions generated by turbulent flows near walls modify the velocity seen by an adhered particle. The transverse velocity of the near wall eddies is about half the streamwise velocity. The near wall vortical motion in this flow was modeled as a plane stagnation point flow by Cleaver and Yates [32] and Fichman *et al.* [33]. An analytical expression for the velocity field was given by Fan and Ahmadi [34], among others. Accordingly, the nondimensional velocity components are given by

$$\begin{aligned} u^+ &= y^+ \\ \upsilon^+ &= -\beta_o y^{+^2}, \quad y^+ \leq 1.85 \\ w^+ &= 2\beta_o y^+ z^+ \end{aligned} \tag{27}$$

In Equation (27), $\beta = 0.01085$ and the dimensionless quantities are defined as

$$\upsilon^+ = \frac{\upsilon}{u^*}, \quad w^+ = \frac{w}{u^*}, \quad y^+ = \frac{u^* \mathrm{y}}{\nu}, \quad z^+ = \frac{u^* \mathrm{z}}{\nu} \tag{28}$$

Here u, υ, and w, respectively, are the fluid velocities in the streamwise, vertical, and spanwise directions, ν is the kinematic viscosity, $u^* = (\tau_w/\rho)^{1/2}$ is the wall shear velocity, τ_w is the wall shear stress, and ρ is the fluid density. In this study the critical shear velocities for particle detachment are evaluated.

The maximum near-wall velocity occurs at $z^+ = \pm \Lambda^+/4$, where $\Lambda^+ = 100$ is the streak spacing. Using Equations (27) and (28) the velocity components at the center of an adhered spherical particle are given as

$$\begin{aligned} u^+ &= \frac{d^+}{2} \\ w^+ &= \beta d^+ \frac{\Lambda^+}{4} \approx \beta \frac{\Lambda^+}{2} u^+ \approx 0.54 u^+ \end{aligned} \tag{29}$$

where

$$d^+ = \frac{d u^+}{\nu} \tag{30}$$

is the nondimensional particle diameter.

Forces and Torques for an Adhered Particle

In this section the forces and torques acting on a particle in contact with a surface in turbulent flow are evaluated. Using Equations (2),

(27), (29), and (30), the expressions for the hydrodynamic moment, drag force, and lift force become

$$M_t = \frac{1.07\pi\rho d_1^3 u^{*2}}{C_c}, \quad F_t = \frac{2.9\pi\rho d_1^2 u^{*2} C_d}{C_c}, \quad F_l = 0.915\rho\nu^2 \left(\frac{d_1 u^*}{\nu}\right)^3 \tag{31}$$

where Equation (2) was used. Similarly, the collision force for carbon dioxide particles becomes

$$F_c = 1.28 E^{*2/5} r^{*1/5} m^{*3/5} V_{cl}^{6/5} \tag{32}$$

CRITICAL SHEAR VELOCITY

Using Equations (12), (25), (31), and (32), the critical shear for rolling detachment is given as

$$u^* = \left[\frac{(F_{po} a)}{B + C}\right]^{1/2} \tag{33}$$

Here B is related to the moments of the hydrodynamic forces and torque acting on the adhered particle which is given by

$$B = \left(\frac{1.07\pi\rho d_1^3}{C_c}\right) + \left(\frac{2.9\pi\rho d_1^2 C_d}{C_c}\right)\left(\frac{d_1}{2} - \alpha_o\right) + \left(\frac{.915\rho u^* d_1^3}{\nu}\right)(a) \tag{34}$$

In Equation (33), C is related to the moment of the impact force on the adhered particle and is given as

$$C = 1.28 \frac{E^{*2/5} r^{*1/5} m^{*3/5}}{u^{*2}} V_{cl}^{6/5} \left[(-\sin\theta)\left(\frac{d_1}{2}\cos\theta + a\right) + (\cos\theta)\left(\frac{d_1}{2}\sin\theta + \frac{d_1}{2} - \alpha_o\right)\right] \tag{35}$$

Using Equations (12), (26), (31), and (32), the critical shear for sliding particle detachment is given as

$$u^* = \left[\frac{\left[F_{po} - \left(\frac{.915\rho u^{*3} d_1^3}{\nu}\right) + 1.28 E^{*2/5} r^{*1/5} m^{*3/5} V_{cl}^{6/5} (\sin\theta)\right] k}{\left(\frac{2.9\pi\rho d_1^2 C_d}{C_c}\right) + 1.28 \frac{E^{*2/5} r^{*1/5} m^{*3/5}}{u^{*2} V_{cl}^{6/5}} (\cos\theta)}\right]^{1/2} \tag{36}$$

For numerical evaluation, Equations (35) and (36) are solved by an iteration scheme. An initial estimate for the critical shear velocity, u^*, was used, and Equations (35) and (36) were iterated until the critical shear velocity converged within 1×10^{-6} m/s.

COMPARISON OF DRAG AND COLLISION FORCES

Since the drag force and the collision force are the two most important forces for particle removal, their relative significance is estimated. The ratio of the nondimensionalized collision force for the case that particles follow the flow is given as

$$\frac{F_c^+}{F_t^+} = \frac{4}{9\pi}\left[\frac{60\pi}{48}\right]^{3/5}\frac{C_c}{f}\left[\frac{E^*}{\rho_f u^{*2}}\right]^{2/5} S^{3/5}\mathrm{Re}^{+8/5}\left[\frac{r_1^*}{d_1}\right]^{1/5}\left[\frac{r_2^*}{d_1}\right]^{9/5} \tag{37}$$

where

$$\mathrm{Re}^+ = \frac{du^*}{v}, \quad S = \frac{\rho_1}{\rho_2} \tag{38}$$

In the derivation of Equation (37), it is assumed that the particles are following the flow and Equation (18) for impact velocity was used.

RESULTS

In this section the results concerning the critical velocity for removal of particles are presented and the magnitude of different forces at the moment of separation are discussed. Unless stated otherwise, it is assumed that the contaminant particles are silicon, the substrate is a silicon wafer, and the nozzle to substrate separation distance is 0.02 m. The corresponding material properties of silicon and solid carbon dioxide are listed in Table 1.

For a carbon dioxide stream in the absence of solid carbon dioxide pellets the critical shear velocities for removal of different size particles by rolling and sliding mechanisms are evaluated and the results shown in Figure 5. It is seen that the critical shear velocities necessary for particle removal increase as the adhered particle diameter becomes smaller. The critical shear velocities necessary for sliding detachment

TABLE I Material Properties of Silicon and Solid Carbon Dioxide

	Silicon	Carbon dioxide pellet
Modulus of elasticity $\left(\frac{N}{m^2}\right)$	1.8×10^{11}	8.9×10^9
Hamaker constant (Nm)	2.35×10^{-19}	N/A
Work of adhesion, W_A $\left(\frac{J}{m^2}\right)$	38.9×10^{-3}	N/A
Density $\left(\frac{kg}{m^3}\right)$	2300	917
Coefficient of friction	0.90	N/A
Poisson's ratio	0.27	0.34

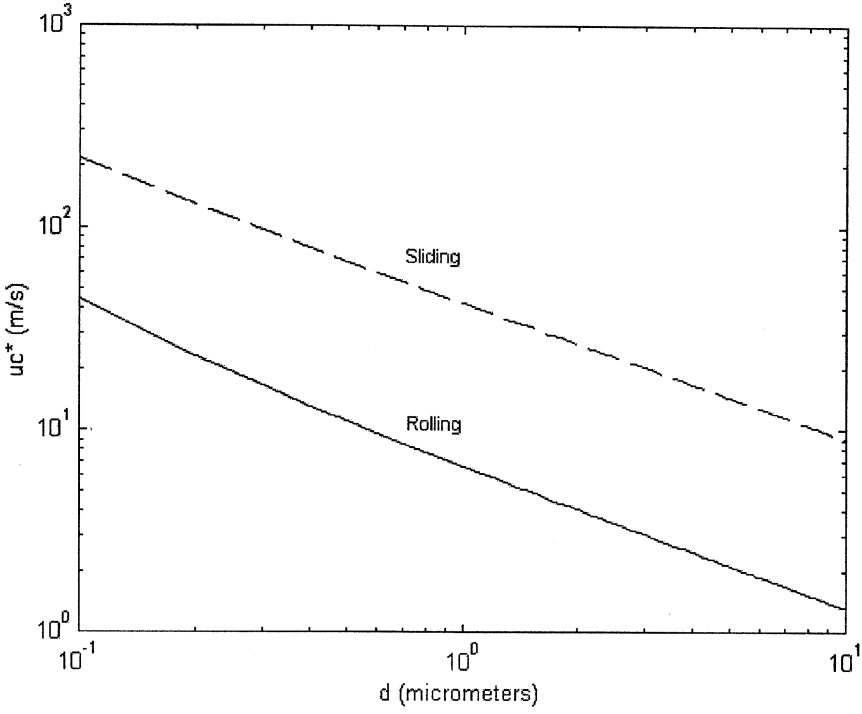

FIGURE 5 Critical shear velocities for silicon particle removal in the absence of carbon dioxide pellets.

are also significantly higher than those for rolling detachment. For example, the critical shear velocity for removal of a 10 μm particle by rolling and sliding mechanisms are 1.3 m/s and 9 m/s (corresponding, respectively, to nozzle velocities of 26 m/s and 180 m/s). For a 0.1 μm particle the critical shear velocities for rolling and sliding removal are, respectively, 45 m/s and 210 m/s (with nozzle velocities of 900 m/s and 4200 m/s).

Figure 6 shows the variations with particle diameter of the drag and lift forces acting on the particle at the moment of separation. Typically, the lift force is an order of magnitude smaller than the drag force. The forces decrease as the adhered particle diameters decrease. The magnitude of forces needed for sliding detachment is also two orders of magnitude larger than those for the rolling removal.

Figure 7 shows the critical shear velocities for removal of contaminant particles in the size range of 0.1 to 10 μm by impact rolling

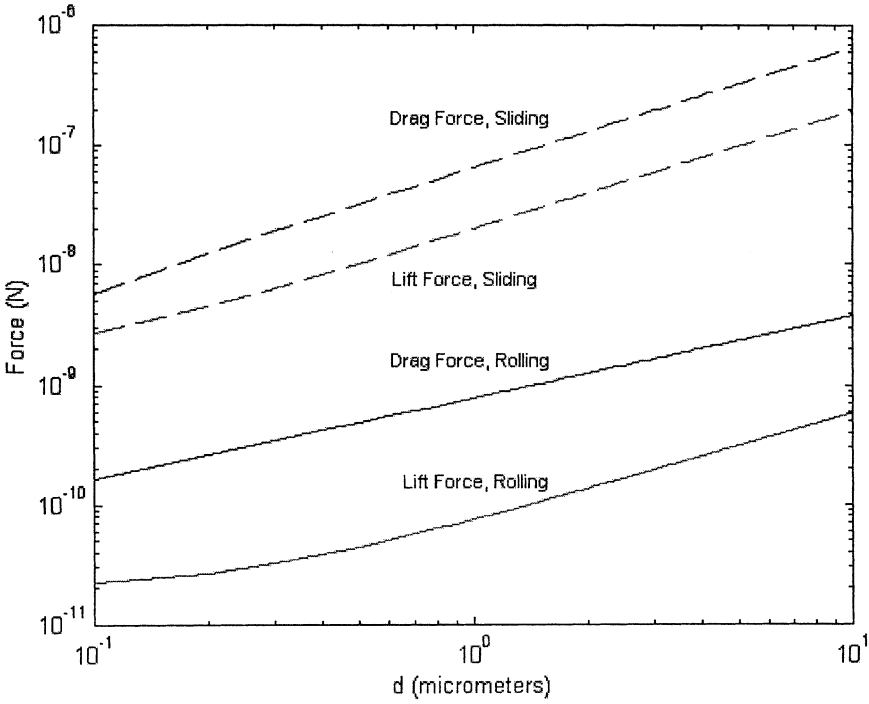

FIGURE 6 Forces at the moment of separation in the absence of carbon dioxide pellets.

and sliding mechanisms for different size impacting CO_2 pellets. The results for typical carbon dioxide pellet diameters in the CO_2 snow, which are between 0.5 μm and 4 μm, are shown in this figure. (It should be emphasized that the carbon dioxide pellets are reduced in size due to sublimation as they travel from the nozzle toward the target surface. This range, however, is expected to cover the expected pellet sizes that are obtained in the current technology.) Here it is assumed that the nozzle is parallel to the substrate, with $\theta = \phi = 0$. This also becomes the case for low nozzle velocities, when the carbon dioxide particles remain suspended in the flow for a long time (before impact), which is several times their relaxation times. The critical removal shear velocities increase as the contaminant particle diameter decreases. While the trends of variations of the removal velocity in Figure 7 are similar to those found in the absence of carbon dioxide pellets, the magnitude of the critical shear velocities for the CO_2 snow are significantly lower.

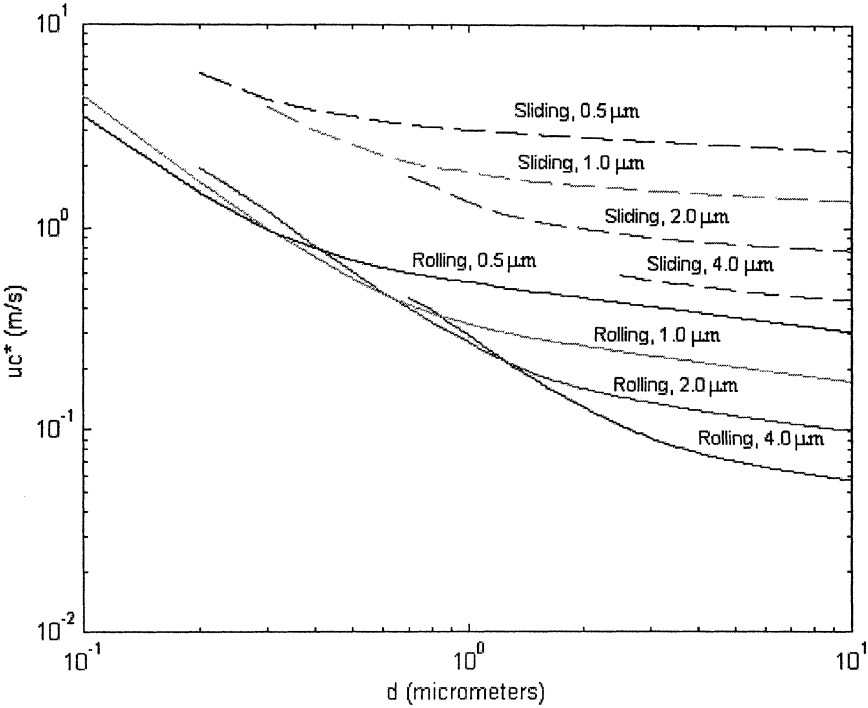

FIGURE 7 Critical shear velocities for particle removal in a cryogenic stream for a horizontal nozzle.

Figure 7 also shows that the removal velocities for impact-sliding detachment are an order of magnitude larger than those for impact-rolling ones. Also, the larger CO_2 pellets are more effective for impact removal of the larger particles but become ineffective for detaching small contaminant particles. For a 10.0 μm contaminant particle, the critical shear velocity for impact rolling and sliding detachment with a cryogenic stream with 0.5 μm carbon dioxide pellets are, respectively, 0.3 m/s and 2.3 m/s. When the cryogenic stream has 4.0 μm carbon dioxide pellets the removal shear velocities drop to 0.06 m/s and 0.45 m/s, respectively. Small 0.1 μm particles, however, can not be removed by the impact-rolling mechanism with CO_2 pellets that are larger than 2 μm. The critical removal shear velocity for cryogenic streams with 0.5 μm and 1 μm carbon dioxide pellets are, respectively, about 3 and 4.5 m/s. That is, the smaller pellets have better chance of removing smaller particles. Figure 7 also shows that particles smaller than 0.2 μm cannot be removed by impact sliding mechanisms. (This is

an important limitation of CO_2 snow surface cleaning, as most contaminant particles are nonspherical and sliding detachment is the only viable mode of removal.)

The critical shear velocities when the nozzle angle is thirty degrees with respect to the substrate are shown in Figure 8. While the general trends of variation are similar to those shown in Figure 7, the critical shear velocities necessary for rolling and sliding detachment are higher. For a cryogenic stream with 0.5 μm carbon dioxide pellets, the critical shear velocities for impact removal of a 10 μm contaminant particle increases by 38% to 3.7 m/s for sliding detachment and by 16% to 0.35 m/s for rolling removal. Similarly, for a CO_2 snow with 4.0 μm carbon dioxide pellets impacting 10 μm contaminants, the critical shear velocity increases by 67% to 0.75 m/s for sliding detachment and 18% to 0.07 m/s for rolling removal. As noted before, larger particles maintain more of their nozzle velocity at impact due to their larger

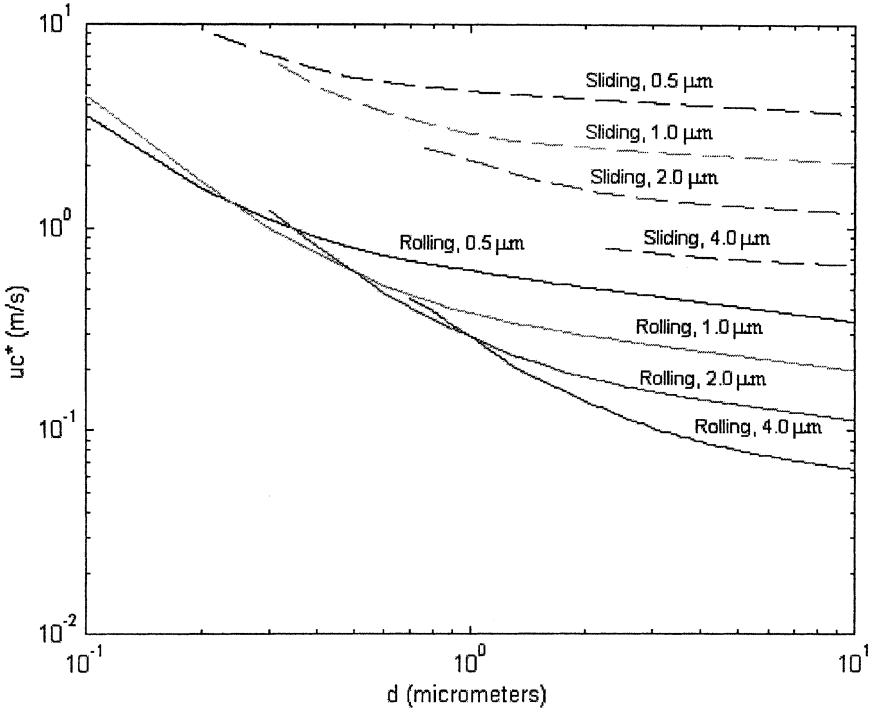

FIGURE 8 Critical shear velocities for particle removal in a cryogenic stream with the nozzle at 30 degrees.

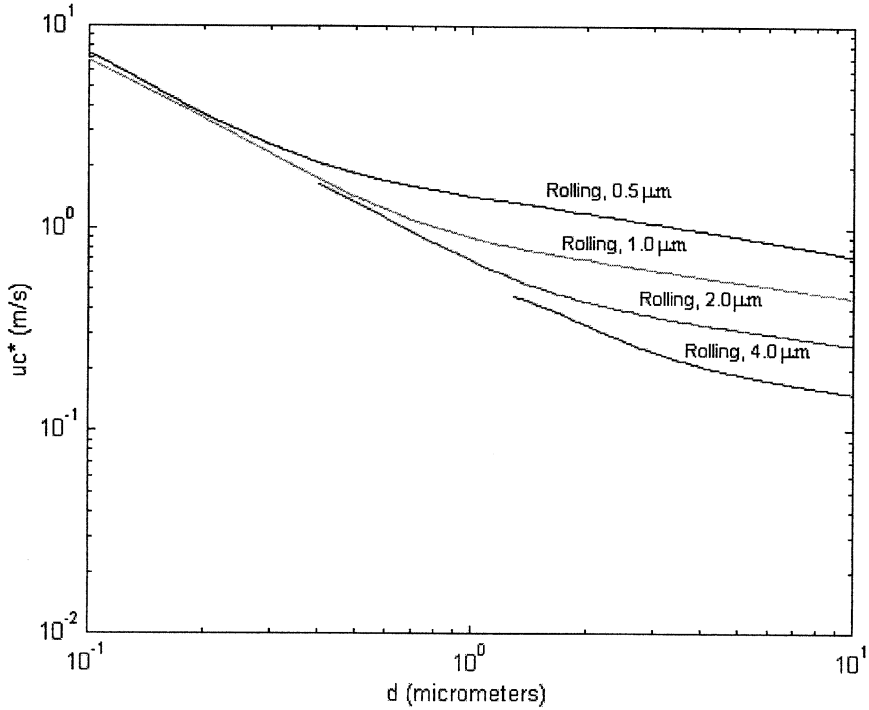

FIGURE 9 Critical shear velocities for particle removal in a cryogenic stream with the nozzle at 70 degrees.

inertia. Therefore, their critical removal velocity is more strongly affected by the nozzle angle.

The critical shear velocities for a nozzle angle of seventy degrees relative to the substrate are presented in Figure 9. The effect of nozzle angle is more clearly seen from this figure. None of the contaminant particles can be removed by the impact-sliding detachment mechanism at this nozzle angle. That is, the vertical component of the impact force is too high to allow the contaminant particle to be detached by sliding. Figure 9 also shows that the critical shear velocities for rolling detachment also increase substantially. For a cryogenic stream with 0.5 μm carbon dioxide pellets, the critical shear velocity for impact-rolling removal of 10 μm contaminant particles increases by 150% to 0.75 m/s when compared with the critical shear velocities at a nozzle angle at zero degrees. The corresponding critical shear velocity for 4.0 μm carbon dioxide pellets also increases by 150% to 0.15 m/s when compared with that for a horizontal nozzle.

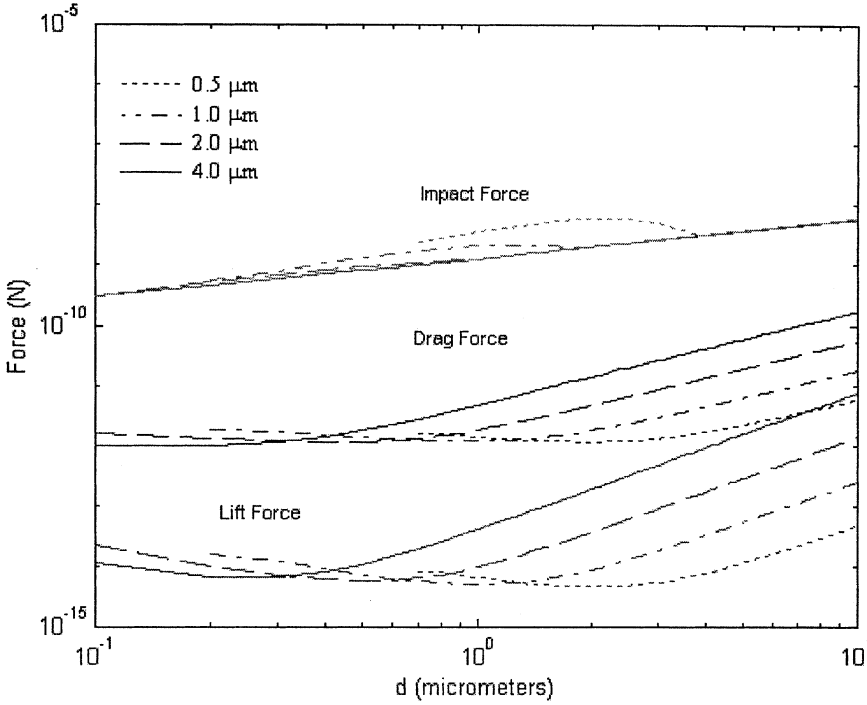

FIGURE 10 Forces at moment of separation for rolling detachment and a horizontal nozzle.

Figure 10 shows the forces at the moment of separation for rolling detachment when the nozzle is parallel to the surface. The impact force is several orders of magnitude larger than the drag and lift forces and is clearly the main force for impact-rolling detachment. The differences between the impact and hydrodynamic forces become even larger for larger carbon dioxide particles. The larger carbon dioxide momentum creates a greater impact force proportional to the volume of the particle, while the drag is proportional to the particle surface area. The effect of impact angle correction due to the geometric constraint can also be observed in Figure 10 by the rise in the impact force.

When the nozzle is parallel to the substrate, the magnitudes of different forces at the moment of separation for sliding detachment mechanism are shown in Figure 11. It is seen that the magnitudes of all forces increase compared with those for the rolling detachment. The impact force is still much larger than the drag and lift forces and

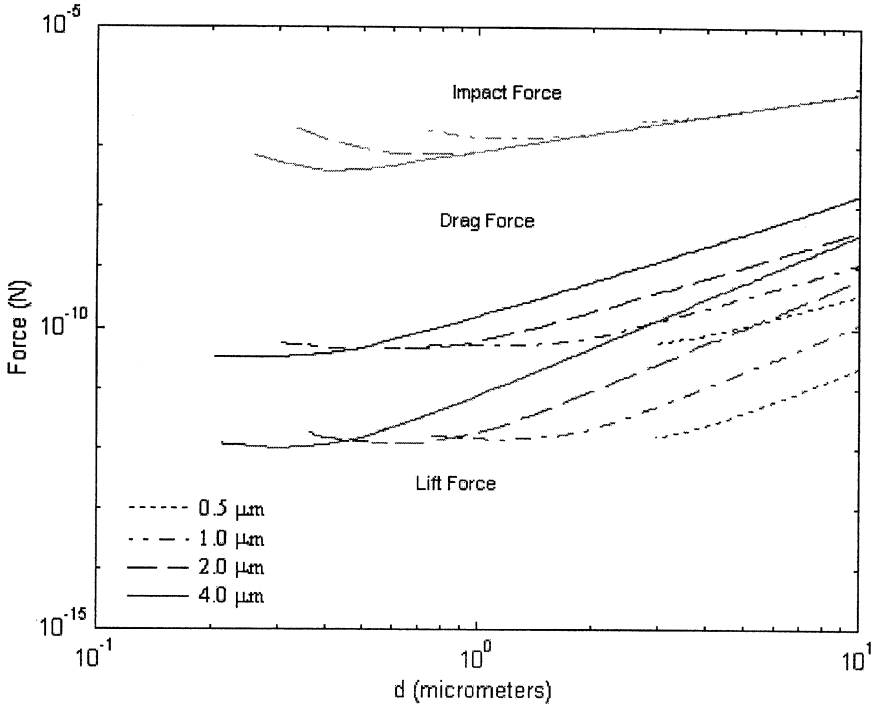

FIGURE 11 Forces at moment of separation for sliding detachment and a horizontal nozzle.

is clearly the main force for impact-sliding removal. The forces also increase as the diameter of carbon dioxide particle increases.

The critical removal shear velocities for a horizontal nozzle at a distance of 0.08 m from the cleaning area is shown in Figure 12. The removal velocities are almost identical to those for the nozzle-substrate distance of 0.02 m shown in Figure 7, particularly for rolling detachment of contaminant particles of larger diameter. There is, however, an increase in the critical removal velocities for impact-sliding removal at larger separation distance. This is because the critical shear velocity for rolling removal of large contaminant particles is rather small, and the carbon dioxide pellets are relaxed to the local flow velocity at short distances from the nozzle. For smaller contaminant particles and sliding removal, however, the removal velocities are larger and the travel distance of the carbon dioxide pellets affects their velocities at impact. Thus, the critical shear velocities are higher for sliding detachment and smaller contaminant

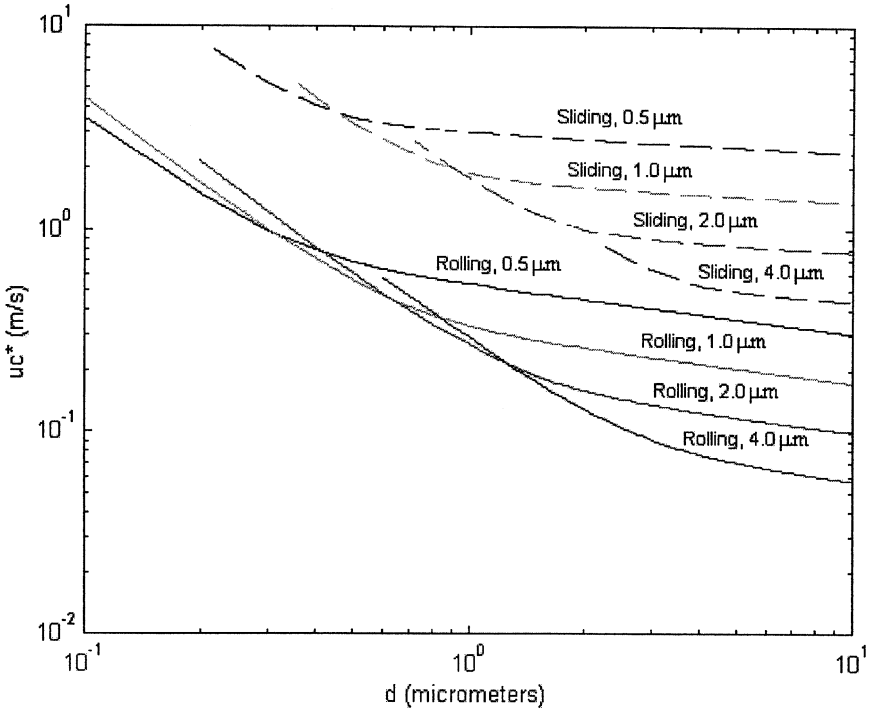

FIGURE 12 Critical shear velocities for cryogenic surface cleaning with a nozzle-substrate separation distance of 8 cm for a horizontal nozzle.

diameters in Figure 12. For example, the critical shear velocity for removing a 0.7 μm contaminant particle by sliding detachment with a cryogenic stream with 0.5 μm carbon dioxide pellets increases by 50%, from 6 m/s to 9 m/s, as the separation distance increases from 0.02 m to 0.08 m. Similarly, the critical shear velocity to remove a 2.5 μm contaminant particle by sliding detachment with 4.0 μm carbon dioxide pellets increases 33%, from 0.6 m/s to 0.8 m/s. The amount of increase in the critical shear velocities for rolling detachment, however, is relatively small.

Figure 13 shows a comparison of the impact and the drag forces at the moment of separation using Equation (37). This figure shows the importance of the impact force on the detachment of the adhered particles. The ratio of the impact force to drag force varies between 35 to 4000 and is generally higher for sliding detachment. The ratio decreases for large particle and for rolling removal of very small particles.

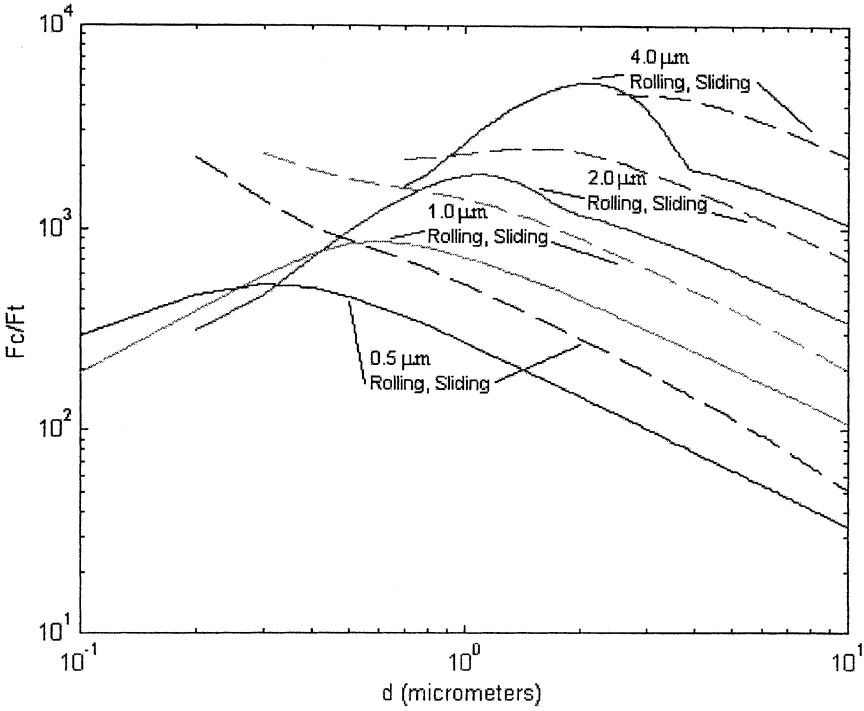

FIGURE 13 Comparison of impact and drag forces for a horizontal nozzle.

As noted before, there is a limitation on the minimum size contaminant particles that are removed by the cryogenic stream containing different size carbon dioxide pellets. For example, for a cryogenic stream with 2.0 μm and 4.0 μm carbon dioxide pellets, the minimum contaminant particle size that can be removed by sliding detachment mechanism are, respectively, 0.7 μm and 2.5 μm. Smaller diameter contaminant particles cannot be removed since the impact force at large impact angle exerts a large normal component. For 0.5 μm and 1.0 μm carbon dioxide pellets, the minimum size contaminant particles that can be removed by sliding detachment are 0.2 μm and 0.3 μm. The minimum sized contaminants removed compares favorably with experimental results obtained by Toscano and Ahmadi [35].

Toscano and Ahmadi [35] reported the results of a series of experiments using a carbon dioxide cryogenic stream for removing calcium sulfate and aluminum oxide from the surface of silicon wafers. The nozzle used generated a sonic cryogenic stream with 3 mm to 5 μm

solidified carbon dioxide pellets at the nozzle outlet. (The carbon dioxide pellet diameters at impact were smaller due to partial sublimation.) Their data showed that the smallest contaminant particles that are effectively removed were about 0.4 μm and 0.5 μm, respectively, for calcium sulfate and aluminum oxide contaminants. The percentage of the particles that are removed also increased as large particle diameter increased. While detailed quantitative comparison is not possible, the experimental removal patterns have the same trends as predicted by the present theoretical model.

CONCLUSIONS

Removal of different size contaminant particles with a carbon dioxide snow stream is studied. Models for impact-rolling and impact-sliding detachments are developed, and the corresponding critical removal velocities for different contaminant and CO_2 pellet sizes are evaluated. On the basis of the results presented, the following conclusions are drawn:

- Impact by the carbon dioxide snow is an effective mechanism for surface cleaning of small and moderate size particles.
- The critical removal velocity for impact-rolling removal is much lower than that necessary for sliding removal.
- Impact removal of large contaminant particles is more easily achieved with a cryogenic stream with a larger solidified carbon dioxide pellets.
- Contaminant particles smaller than a certain size cannot be removed with a cryogenic stream with carbon dioxide pellets larger than a certain diameter.
- Effective removal of very small particles requires cryogenic streams with very small carbon dioxide pellets. (Design modification of current technology is needed in this regard.)
- The effectiveness of cryogenic surface cleaning increases as the nozzle-substrate angle decreases. The angle effect is more important for larger carbon dioxide pellets and contaminant particles. The angle effect becomes negligible for small CO_2 pellets that impact with local fluid velocity.
- Increasing the nozzle-substrate separation distance slightly increases the critical velocity needed for particle removal. The effect of the changes in the separation distance becomes noticeable only if it is sufficiently large to affect the level of the relaxation of particle velocity to the local flow velocity.

The presented results indicate that the impact removal mechanics can explain the effectiveness of cryogenic surface cleaning process. While the other mechanisms such as phase change, rapid evaporation, etc., could contribute to surface cleaning, the impact of carbon dioxide pellets appears to be the main cause of dislodging the adhered particles.

REFERENCES

[1] Hoenig, S. A., "Cleaning Surface with Dry Ice." *Compressed Air Magazine*, **7**, 12 (1986).
[2] Hoenig, S. A., "Dry Ice Snow as a Cleaning Media for Hybrids and Integrated Circuits." *Hybrid Circuit Technology*, **7**, 34 (1990).
[3] Jackson, D. and Carver, B., "Today's Forecast: It Looks Like Snow." *Precision Cleaning*, **8**, 17–29 (1999).
[4] Corn, M., "Adhesion of Particles." *J. Aerosol Science*, 359 (1966).
[5] Krupp, H., "Particle Adhesion. Theory and Experiment." *Adv. Colloid Interface Sci.*, **1**, 111–140 (1967).
[6] Visser, J., "On Hamaker Constants: A Comparison Between Hamaker Constants and Liftshitz-Van Der Waals Constants." *Adv. Colloid Interface Sci.*, **3**, 331–363 (1972).
[7] Tabor, D., "Surface Forces and Surface Interactions." *J. Colloid Interface Sci.*, **58**, 2–13 (1977).
[8] Bowling, R. A., "An Analysis of Particle Adhesion on Semiconductor Surfaces." *J. Electrochem. Soc.*, **132**, 2208–2219 (1985).
[9] Ranade, M. B., *J. Aerosol Sci. Technol.*, **7**, 161–176 (1987).
[10] Soltani, M. and Ahmadi, G., "On Particle Adhesion and Removal Mechanisms in Turbulent Flows." *J. Adhesion Sci. Technol.*, **8**, 763–785 (1994).
[11] Hamaker, H. C., "The London-Van der Waals Attraction Between Spherical Particles." *Physica*, **4**, 1059–1072 (1937).
[12] Lifshitz, E. M., "The Theory of Molecular Attractive Forces Between Solids." *Soviet Phys., JETP*, **2**, 73–83 (1956).
[13] Derjaguin, B. V., "Untersuchungen Über Die Reibung and Adhäsion, IV." *Kolloidn. Zhur.*, **69,** 155–164 (1934).
[14] Johnson, K., Kendall, K. and Roberts, A. D., "Surface Energy and Contact of Elastic Solids." *Proc. R. Soc., London*, **324**, 301–313 (1971).
[15] Derjaguin, B., Muller, V. and Toporov, Y., "Effect of Contact Deformations on the Adhesion of Particles." *J. Colloid Interface Sci.*, **53**, 314–326 (1975).
[16] Muller, V., Yushenko, V. and Derjaguin, B., "On the Influence of Molecular Forces on the Deformation of an Elastic Sphere and Its Sticking to a Rigid Plane." *J. Colloid Interface Sci.*, **77**, 91–101 (1980).
[17] Muller, V., Yushenko, V. and Derjaguin, B., "General Theoretical Consideration of the Influence of Surface Forces on Contact Deformations and the Reciprocal Adhesion of Elastic Spherical Particles." *J. Colloid Interface Sci.*, **92**, 92–101 (1983).
[18] Layden, L. and Wadlow, D., "High Velocity Carbon Dioxide for Cleaning Vacuum System Surfaces." *J. Ac. Sci. Technol.*, **8**, 3881–3883 (1990).
[19] McDermott, W., Ockovic, R., Wu, J., Cooper, D., Schwartz, A. and Wolfe, H., "Surface Cleaning Using a Cryogenic Aerosol." US Patent No. 5,062,898. (1991).
[20] McDermott, W., Ockovic, R., Wu, J. and Miller, R., "Surface Cleaning by a Cryogenic Argon Aerosol." *Proceedings Institute of Environmental Sciences*, 8882–8885 (1991).

[21] Loveridge, R., "CO_2 Jet Spray Cleaning of IR Thin Film Coated Optics." *Proceedings of Society for Optical Engineering*. July 25–26, 1991.
[22] John, W., Fritter, D. and Winklmayr, W., "Resuspension Induced by Impacting Particles." *J. Aerosol Sci*., **22**, 723–736 (1991).
[23] John, W. and Sethi, V., "Breakup of Latex Doublets by Impaction." *Aerosol Science and Technology*, **19**, 57–68 (1993).
[24] Kohli, R., "Nonaqueous Processes Provide Critical Cleaning Alternatives." *Precision Cleaning*, **5**, 19–23 (1997).
[25] Wang, C., Chang, R., Lin, W., Lin, R., Liang, M., Yang, J. and Wang, J., "Supercritical CO_2 Fluid for Chip Resistor Cleaning." *J. of the Electrochemcial Society*, **146**, 3485–3488 (1999).
[26] Narayanswami, N., "A Theoretical Analysis of Wafer Cleaning using a Cryogenic Aerosol." *J. of the Electrochemical Society*, **146**, 767–774 (1999).
[27] O'Neill, M., "A Sphere in Contact with a Plane Wall in a Slow Linear Shear Flow." *Chem. Eng. Sci*., **23**, 1293–1298 (1968).
[28] Saffman, P. G., "The Lift on a Small Sphere in a Slow Shear Flow." *J. Fluid Mechanics*, **22**, 385–395 (1965).
[29] Fan, S. L. and Zhu, C., *Principles of Gas-Solid Flows* (Cambridge University Press, Cambridge, 1998).
[30] Tsai, C. J., Pui, D. Y. H. and Liu, B. Y. H., "Particle Detachment from Disk Surfaces of Computer Disk Drives." *J. Aerosol Sci. Technology*, **22**, 737–746 (1991).
[31] Wang, C., "Effects of Inceptive Motion on Particle Detachment." *Aerosol Sci. Technol*., **13**, 386–396 (1990).
[32] Cleaver, J. W. and Yates, B., "A Sub Layer Model for the Deposition of Particles from a Turbulent Flow." *Chem. Eng. Sci*., **30**, 983–992 (1975).
[33] Fichman, M., Gutfinger, C. and Pnueli, D., "A Model for Turbulent Deposition of Aerosols." *J. Aerosol Sci*., **19**, 123–136 (1988).
[34] Fan, F. and Ahmadi, G., "A Sublayer Model for Turbulent Deposition of Particles in Vertical Ducts with Smooth and Rough Surfaces." *J. Aerosol Sci*., **24**, 45–64 (1993).
[35] Toscano, C. and Ahmadi, G., "Experimental Study of Particle Removal in Cryogenic Surface Cleaning." *J. Adhesion* (to be submitted) (2003).